IIETA International Information and Engineering Technology Association
Advancing the World of Information and Engineering

Traitement du Signal
Vol. 40, No. 3, June, 2023, pp. 1107-1117
Journal homepage: http://iieta.org/journals/ts

An Examination Monocular Vision Gaze Point Tracking under the Theory of 'Machines Displacing Workers' in the Philosophy of Technology

Haijun Zhou[1,2], Wei Chen[3], Zimin Lin[4], Ruiyang Chen[5,6*]

[1] Department of Audit, Zhejiang College of Security Technology, Wenzhou 325000, China
[2] School of Marxism, Northwestern Polytechnical University, Xian 710072, China
[3] Logistics Service Department, Wenzhou Business College, Wenzhou 325035, China
[4] Department of Planning and Finance, Zhejiang College of Security Technology, Wenzhou 325000, China
[5] School of Marxism, Wenzhou Medical University, Wenzhou 325000, China
[6] School of Marxism, Zhejiang University, Hangzhou 310000, China

Corresponding Author Email: chenruiyang@wmu.edu.cn

https://doi.org/10.18280/ts.400326

Received: 10 March 2023
Accepted: 20 May 2023

Keywords:
machines displacing workers, monocular machine vision, gaze point analysis, CarSim, ambient lighting, lighting-attention quantitative model

ABSTRACT

With the continuous development of technology, we have the opportunity to quantitatively study the internal behaviors of personnel, such as attention, in a suitable way, in order to better solve the "machine compensation" for workers and achieve the development of human-machine fusion. An exploration of how varying lighting conditions directly affect the eyes and, by extension, the individual's attention has been undertaken in this study. Image sensors capture the subject's eye movements during task participation, with the location of the eye's (pupil's) center aiding in gaze point recognition and facilitating the quantification of attention. A quantifiable model of "lighting-attention" has been developed through controlled lighting conditions and replicable experimental circumstances, thereby studying the alteration of attention under different lighting and road conditions. An initial calibration of a monocular vision gaze tracking system was achieved with two commercial-grade eye trackers and calibration software, achieving a precision level of 2 cm. Nine college students aged 20-21, divided into male and female control test groups, exhibited similar attention characteristics under various lighting conditions. Overall, a negative correlation between illumination intensity and attention is observed when exceeding a certain threshold. On average, female participants maintained higher attention levels for longer durations. The efficacy of the model proposed in this study has been proven through a series of tests, providing a quantifiable reference for the mechanisms influencing attention. So it can provide the basis for the study of the benefits of factory workers.

1. INTRODUCTION

The Philosophy of technology in the era of artificial intelligence is the coexistence of opportunities and risks. With the continuous progress of technology and the deepening of automation, especially the breakthrough development of artificial intelligence technology represented by OpenAI this year, the theory of "machines displacing workers" has once again attracted widespread attention and discussion in recent years [1]. The core of this theory is "Automation and Employment", which was first proposed in the 1950s. Economists such as John Maynard Keynes and Nobel laureate Paul Samuelson have proposed or commented on this theory [2]. Smarter AI can further liberate people from mechanical labor to improve production efficiency, but this will have an impact on the existing employment environment and work structure [3]. Both office clerks and software blue-collar workers seem to be worried about weakening or losing their jobs under the impact of AI technology. Even when Level 4 autonomous driving systems can be "popularized" at a price of US$30,000, more than 160 million drivers around the world actually feel the pressure [4]. However, machines themselves cannot speak and cannot tell us how they understand reality. They are more like the intelligent extension of AI designers. This "limited communication" cannot fully understand the true intentions behind the actual complex operations. With the continuous development of technology, we have the opportunity to quantitatively study the internal behavior of personnel, such as attention, in a suitable way, so as to better solve the problem of "machine compensation" for workers and achieve human-machine integration development.

The adage, "The eyes are the window to the soul," brings two significant issues to light [5]. Firstly, it emphasizes the fact that a substantial portion of human information intake is facilitated through the eyes. Secondly, it suggests that invisible psychological activities in humans can be reflected through the eyes and the gaze [6]. This proposition gives rise to research into quantitatively modeling attention by tracking and quantifying eye usage. Disregarding complex psychological activities and focusing solely on the entities themselves, it is critical to acknowledge that lighting directly influences human attention. This is because, through prolonged evolution, humans have adapted to form an internal clock, or circadian rhythm, that synchronizes with the 24-hour rotation of the Earth, marked by changes in light and dark [7].

Studies conducted by Kamali and Abbas [8] have unveiled

that light is an indispensable mechanism for bodily function regulation, including sleep and alertness [9]. Under the influence of light, crucial hormones like melatonin [10] and cortisol [11] are produced. These hormones play a vital role in healthy rest-activity patterns [12] and are of utmost importance for cognition and emotions [13]. Illumination plays an essential role in daily life, making it indispensable for optimal functioning across varied environments. Therefore, it is apt to say that lighting directly influences every aspect of human existence. Tanner [14] reiterated, "After food and water, light is the most crucial environmental input for body function regulation."

To compensate for the insufficiency of natural light or due to the constraints of the work environment, artificial lighting systems have been a crucial part of human production and life since ancient times. Particularly since the Industrial Revolution, artificial lighting has demonstrated its ability to partially compensate for stabilizing the body, mind, and emotional processes [13, 14]. Therefore, in architectural design, the importance of lighting design, including natural daylighting and indoor lighting, is on par with the significance of space utilization [15]. Different lighting conditions have a relatively significant impact on individual learning outcomes. When light reaches cells like photopigments through the eyes [16], complex chemical reactions occur, thereby affecting cognitive performance, such as learning and attention [17]. An estimation made by Dember and Neiberg [18], and they indicate that about 20% of children entering school encounter visual problems. Statistical-based studies have demonstrated a strong correlation between lighting design and individual attention. However, due to the joint effects of the test subject and various environmental factors, it is often difficult to quantify the strength of this impact, which makes it more objective and intuitively demonstrates this relationship. Rasinski et al. [19] quantified attention through Oral Reading Fluency (ORF) and tested it with standard or customized reading checklists (IRI) to express the impact of lighting on reading.

However, this method is still influenced by the ability of the test subjects and is challenging to be directly applied to other scenarios such as popular artificial intelligence and autonomous driving. Utilizing Electroencephalogram (EEG) equipment, extremely comprehensive and precise attention-related data can be obtained [20]. Yet, stringent testing environments and high costs have limited the mass development of such equipment [21, 22]. This has steered attention-related research towards machine vision-focused research proposals. Zheng et al. [23] have studied the robust algorithm for extracting eye features (pupil center and radius, canthus, and eyelid contour) from frontal face images. Considering various factors like illumination, infrared, glasses, and test distance, most currently prefer using multiple cameras and infrared light sources. For instance, a novel dual-camera gaze detection system was proposed by Park et al. [24], using infrared LED lights to provide light sources for wide-angle and telephoto cameras. This simplifies the detection of facial features, pupil, and iris positions. A binocular gaze detection-based eye tracking system, including three miniature cameras and two infrared lenses for user observation, was introduced for user's region of interest extraction [25]. With further advancement, commercial-grade eye trackers have been developed, such as Tobii Eye [26], Tobii Pro Glasses [27], and aSee Pro desktop eye movement analysis [28].

To uncover the impact and intrinsic correlation of human attention under different lighting environments, a more straightforward monocular vision gaze point tracking method was designed for the quantification of human gaze under different lighting conditions. Based on this, a "light-attention" quantitative model was established using gaze point (focus) data, referencing the ORF model, and the Root Mean Square Error was utilized to evaluate the relationship between attention and illumination. In the experimental validation, a CarSim-based attention testing environment was designed to obtain the attention change data of the subjects under different testing conditions. This validates the effectiveness of the "light-attention" quantitative model and provides a quantitative reference for the mechanism of human attention influence.

2. MONOCULAR VISUAL FOCAL POINT LOCALIZATION METHOD

2.1 Overview

The methodology for monocular vision focus localization can be generally divided into three components: face and eye detection, eyeball center localization, and focus calculation. The structural framework for the eye movement tracking algorithm is shown in Figure 1.

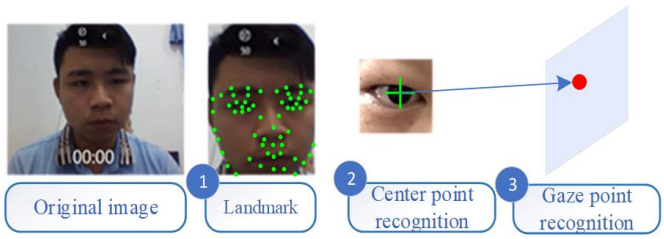

Figure 1. Eye movement tracking algorithm framework

2.2 Eye detection

Facial Landmark Detection (FLD) [29] can be employed directly for identifying facial features within a scene. An added benefit of the FLD method is its capacity to generate features points directly. The Dlib standard library offers 68 feature points, with identifiers 37-40 and 43-46 representing the left and right eyes, respectively [30]. This undeniably simplifies the implementation of eye tracking [31]. More details on the Dlib library and its implementation can be found in the study [32].

2.3 Calculation of eye center localization

The eye presents distinct characteristics, and geometrically, it can be approximated as a sphere, its projection taking a circular shape (as shown in Figure 2) [33]. Thus, the center of the circular target (the eye) can be detected by analyzing the vector field of the image gradient [34]. This research presents a method for eye center detection, which is based on an image gradient vector field representation, as illustrated in Figure 2.

Figure 2 demonstrates the detection method's results with (a) a deviation present, and (b) results that meet expectations. A light background is used to simulate the sclera, with a dark area simulating the iris. Let c be a possible center and provide the gradient vector at location X_i. Subsequently, the normalized displacement vector d_i should have the same

direction as the gradient g_i. For instance, in Figure 2(a), the displacement vector d_i and the gradient vector g_i do not share the same direction, and c implies a deviation from the actual center; while in Figure 2(b), d_i and g_i have the same direction, suggesting that c' overlaps with the actual center.

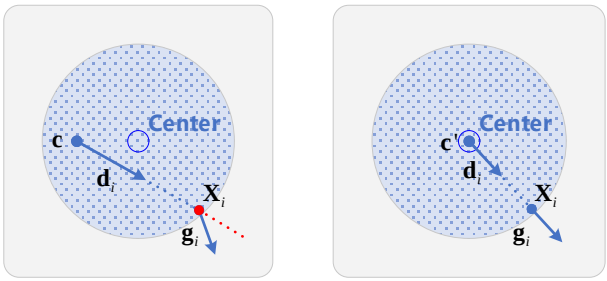

(a) Presenting deviation (b) Meeting expectations

Figure 2. Example of eye center detection method based on image gradient vector field

The vector field based on image gradient can be utilized for calculating the dot product between the normalized displacement vector and the gradient vector g_i. At this point, the optimal center x^* of circular objects in the image can be expressed as follows

$$c^* = \arg\max_c \left\{ \frac{1}{N} \sum_{i=1}^{N} \left(d_i^T g_i \right)^2 \right\} \tag{1}$$

$$d_i = (x_i - c) / \|x_i - c\|_2, \forall i : \|g_i\|_2 = 1 \tag{2}$$

where, the displacement vector d_i is scaled proportionally to unit length to ensure equal weight at all pixel locations. An example evaluation of the dot product sum for different centers is depicted in Figure 3, where Figure 3(b) shows a strong maximum of the objective function at the center of the pupil.

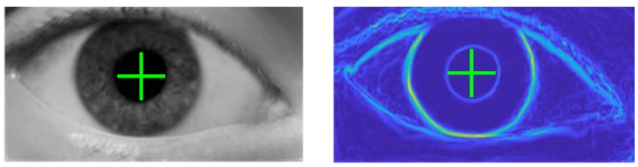

(a) Pupil center (b) Mesh image

Figure 3. Evaluation schematic

However, the presence of interference objects around the eye, such as hair, skin, and glasses, leads c to a bias towards local maxima, causing c a deviation from the actual center. To address this, the colors of the iris, skin, and pupil can be selected as prior knowledge ω_c to enhance distinction, as the pupil color tends to be darker. A weight ω_c can be applied to each possible center c, allowing darker centers c to have a higher possibility of being the actual center. Consequently, the objective function can be updated.

$$\arg\max_c \frac{1}{N} \sum_{i=1}^{N} \omega_c \left(d_i^T g_i \right)^2 \tag{3}$$

After smoothing the input image I_{in} (e.g., through a low-pass Gaussian filter) and then reversing it to emphasize the dark pupil area, the grayscale value ω_c at the $c(x, y)$ coordinate position can be determined. Ultimately, due to the trilinkage of the eyes [35], the centers of the two eyes $\boldsymbol{c}_l$ and $\boldsymbol{c}_r$ validate each other. When $\Delta|c_l - c_r| < 0.25$, the centers are found to be consistent, it is considered reliable, thereby enhancing accuracy and anti-interference ability.

The accuracy of the eye center inspection method was validated using the BioID dataset in the tests [36], and in conjunction with the Dlib library, an average accuracy rate of over 95% was achieved in the tests.

2.4 Gaze point detection

Figure 4 illustrates the method of gaze detection in three-dimensional space, defining the intersection of the gaze line and screen as the gaze point Q. A virtual gaze plane, orthogonal to the line OP and passing through the camera O, is initially denoted as plane H. This plane H rotates in accordance with the 3D pupil position. The X'-axis on plane H encompasses the camera O, and is formed by the intersection line between plane H and the horizontal plane of the global coordinate system. The intersection point between plane H and the line PQ is represented as T. The angle between the line OT and the X'-axis is denoted as φ.

The angle between OP and PQ is defined as θ. The coordinates of point T on plane H exhibit a one-to-one correspondence with the combination of φ and θ, θ=θ' and $\theta = f(|\boldsymbol{r}|)$, where, r is the vector from the corneal reflection center to the pupil center in the captured image; φ is the declination of the vector r in plane, which is parallel to the camera image sensor and passes through the center P of the eye, and φ is compensated by the camera attitude determined by the camera calibration. Thus, the coordinates of point T on plane H can be computed from $|r|$ and φ. The optic axis of the eye is determined by connecting points P and T on the global coordinate system. The gaze point Q is detected as the intersection of the optic axis and the screen.

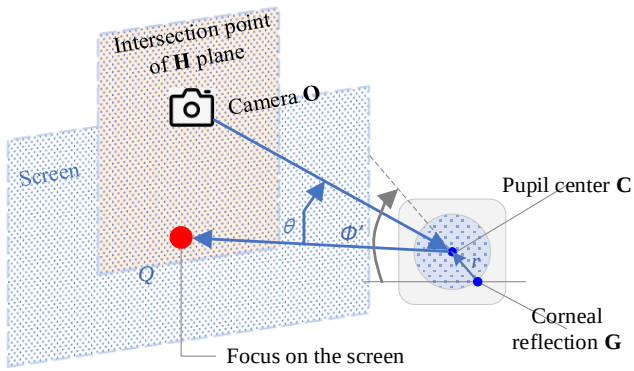

Figure 4. Principle of gaze point detection

3. ATTENTION QUANTIFICATION MODEL (AQM）

3.1 Attention testing system

The AQM adopts the "Car Simulation Driving [37]" simulation system, CarSim, as the experimental carrier for the research of attention quantification of the subjects tested. This choice stems from the inherent necessity for highly concentrated attention in car driving. As shown in Figure 5, the entire experimental system consists mainly of two parts: the CarSim system and the attention recognition system.

It is observed that the focus of the test subject should be

concentrated on the road in front of the cockpit. Thus, attention is converted into the line-of-sight focus of the test subject. Current methods for obtaining the line-of-sight focus of the test subject fall into two categories: the machine vision-based eyeball tracking system under visible light environment and the infrared-based eyeball tracking system like Tobii Eye [26]. This study opts for the monocular vision focus positioning method, primarily due to the following reasons:

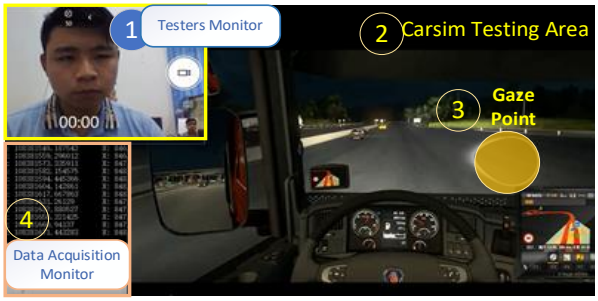

(a) The testing system interface

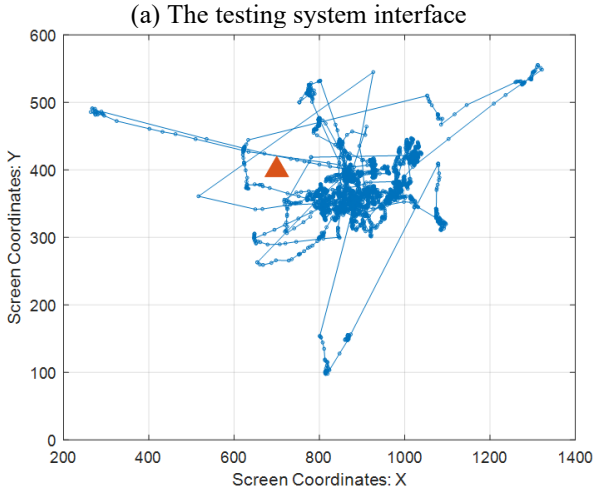

(b) The visualization of focus data

Figure 5. Attention testing system: CarSim simulator

Currently, most of the line-of-sight estimation techniques use the Pupil-Cornea Reflection method (PCCR) [38] which necessitates an additional auxiliary light source. The user is required to keep the head relatively still during use and the deployment of potentially impacting, high-cost external devices on the subject is necessary [27]. Utilizing the built-in camera of a laptop or adding an inexpensive network camera to a PC can implement eyeball tracking and focus positioning at a very low cost and on a large scale.

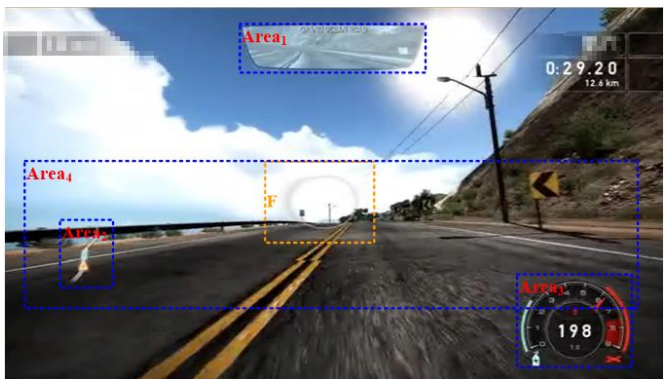

Figure 6. Quantified UI simulation view [35]

3.2 Setting of attention testing area

In order to facilitate the quantification of the aforementioned experimental system using a mathematical model, as shown in Figure 6, the CarSim screen [39] of this study is decomposed into several test areas $A = \{a_1, a_2, \cdots, a_n\}$. Considering the real environment, there are mainly the following types of areas: the main window, which is the visible area of the front windshield; the left and right rearview mirror areas; the internal rearview mirror area; the dashboard; the invalid area and other areas that do not need temporary attention.

For these areas, a weight coefficient w_i is assigned according to their importance, and $\sum_{i=1}^{n} w_i = 1$. The weight of the invalid area a_1 is obviously $w_1 = 0$. The setting of the weights is due to the fact that, according to the general behavior of personnel, it is unlikely that the driver will focus their line of sight on the rearview mirror and dashboard for a long time. It is reasonable to focus on these locations momentarily or short-term. Usually, most of the time should be on the main window, that is, on the road, otherwise vehicle deviation will occur, and even a car accident may occur. Based on this consideration of simulating real conditions, the aforementioned visual areas are divided into four parts: 1) the invalid area $A_{ERR} = \{a_1, a_2, \cdots, a_x\}$; 2) the main road area $A_{road} = \{a_{x+1}, a_{x+2}, \cdots, a_y\}$; 3) the rearview mirror area $A_{RV} = \{a_{y+1}, a_{y+2}, \cdots, a_m\}$; 4) the dashboard area $A_{DB} = \{a_{m+1}, a_{m+2}, \cdots, a_n\}$. Similarly, the weight coefficients of each area are set, the road area $w_{road} = 0.95$, the rearview mirror $w_{RV} = 0.035$, and the dashboard $w_{DB} = 0.015$.

The gaze point is defined as $F(P)$, then the line-of-sight window can be defined as $Area_F = (List\langle P\rangle)$. The gaze points raw data obtained in Chapter 2 is position data. After mapping and converting to the screen coordinate system, it still maintains a real number definition, that is, a real number of $F(\text{Point}(x, y))$ structure. In this way, a single sample can be defined as $s(t, F)$, that is, the gaze position F at time t, then the m sample sequence can be represented as:

$$S = \{s_1(t, F_1), s_2(t, F_2), \cdots, s_m(t, F_m)\} \tag{4}$$

In this way, based on Eq. (4), after eliminating invalid points, the sample sequences in each area can be cumulatively calculated to achieve the quantification of attention.

3.3 Attention quantification method

The concept of attention, although prone to changes influenced by external environment and internal psychological activities, maintains its thematic target characteristics under a specific task theme. Taking driving activity as an example, the overall driving behavior is essentially conducive to safety. This attention process is time-variant and may not necessarily be continuous, but it should generally meet reasonable requirements. For instance, observing the rearview mirror is typically considered normal; however, if a driver "long-term" focuses on the rearview mirror, this behavior transitions from "normal" to "abnormal". Therefore, this "abnormal behavior" can be defined as a lack of attention.

Definition 1: For the effective window set *Area*, if the line-of-sight condensation point F is not within the *Area* range in time Δt, then an attention abnormality is considered to have occurred.

Based on Definition 1, an attention abnormality detection framework can be constructed, and in combination with the Attention Quantification Model (AQM), the changes in attention and inherent mechanism under different conditions, such as illumination effects, can be understood. The attention abnormality detection framework is shown in Figure 7.

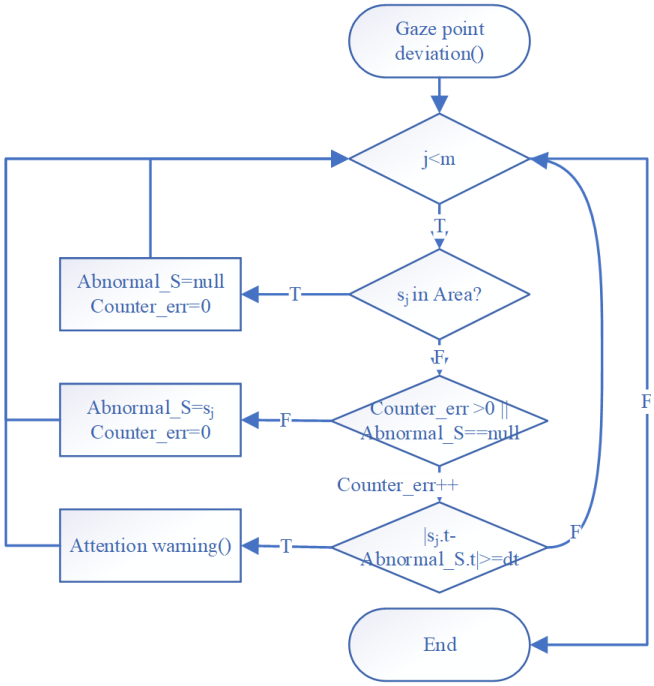

Figure 7. Attention anomaly detection framework

3.4 Attention error model

Rasinski et al. [19] in the ORF test defined attention as Q, which is the ratio between the number of correctly read words W_R and the total number of words W_T, that is:

$$Q = \frac{W_R}{W_T} \times 100\% \tag{5}$$

It is known that $Q \in [0,100\%]$, when $Q = 100\%$, the subject's attention is highest.

In this study, to simplify the sampling process, the sampling frequency of the eye movement analyzer is set to F (the error in actual sampling is less than 5%), thus, $C_{Total} = F * T_s$ focus samples can be obtained in the test time T_s. These samples are distributed in four test areas, and the number in each area is c_i, respectively, then:

$$C_{Total} = F * T_s = \sum_{i=1}^{n} c_i = c_{ERR} + c_{road} + c_{RV} + c_{DB} \tag{6}$$

Therefore, referring to Eq. (5), the Attention Quantification Model in this study can be defined as:

$$Q^{'} = \frac{c_{ERR} * w_{ERR} + c_{road} * w_{road} + c_{RV} * w_{RV} + c_{DB} * w_{DB}}{C_{total}} \times 100\% \tag{7}$$

According to the area weight coefficient set in section 3.1, by substituting it into Eq. (7), it can be seen that the ideal attention value that complies with reality should be 90.395%. When it is higher than this value, it indicates that the driver pays excessive attention to the road conditions and ignores the situation of other vehicles behind the vehicle, as well as the condition of the vehicle itself; when it is lower than this value, it indicates that the driver's attention may be distracted, and the risk at this time is higher than the former.

3.5 Illumination-attention relationship model

Given that illumination intensity can be measured, and the attention value of the test subjects can be identified based on Eq. (4), it is plausible to establish an Illumination-Attention Relationship Model. Existing research and common knowledge suggest that attention tends to decline when the illumination is too strong or too weak. However, attention reaches a relatively high level under appropriate illumination conditions. This relationship can be expressed by a polynomial. If the illumination intensity at a measured position p is defined as I_p, and the attention of the subject at this position is Q_p, their relationship can be expressed as:

$$Q_p = 1.503\text{e-}07\left(I_p\right)^3 - 1.756\text{-}04\left(I_p\right)^2 + 0.0417 I_p + 86.46 \tag{8}$$

Since there are no other referential studies and conditions to solve Eq. (8), an approximate solution is sought through experimental data in this study. By substituting the test results of section 4.5 into Eq. (8) and selecting RMSE as the error evaluation index, polynomial coefficients can be obtained. The optimal result is obtained when the cubic polynomial RMSE equals 2.9688.

4. TESTING AND RESULT ANALYSIS

4.1 Setting of building and illumination environment

An open-plan experimental lab was selected as the testing location, the basic structure of which is represented in Figure 8.

Figure 8. Architectural layout of the experimental site

The test site is an independent classroom, unconnected to other classrooms, with specific architectural parameters: 1) The exterior dimensions of the classroom are approximately 8.4m (L) and 7m (W). 2) The dimensions of the floor tiles and the suspended ceiling within the classroom are 0.60.6m, dividing the room into 1411.5 units. 3) The classroom is arranged in a north-south layout. The north side features a dimension of 2.4 (L)1.2 (H) m (due to the blockage of the blackboard, the actual size is 2.40.8m), as well as a typically closed internal double door of 2.05 (L)*1.4 (H) m; on the south side, there are two sliding windows each with dimensions of

1.8 (L)*1.7 (H) m. Due to the obstruction of indoor furniture, the effective daylighting size of the two windows is 2.7 (L)*1.7 (H) m. Throughout the test, the curtains remained open. 4) The classroom ceiling is uniformly equipped with 9 modular fluorescent lights. Each module is fitted with three 18W 0.6m fluorescent tubes, model FSL T8-18W. It should be noted that two of the modules, due to malfunction, only have one working tube. 5) There are open corridors of 2.2m width in the north and south of the classroom, with the corridor lights remaining off during the test.

Furthermore, the arrangement of furniture and equipment within the test site maintained their regular placement, providing more realistic test conditions and environments. A familiar environment assists in reducing any discomfort for the tested students, as well as psychological changes.

4.1 Time period and illumination collection

The illumination was measured using the VICTOR 1010D digital lux meter [40], with illuminance levels taken at 20 points, as shown in Figure 9. Illumination at points 1 to 16 is representative, while data from points 17 to 20 aid in addressing the issue of negative illumination at the edges of the regions in subsequent data analysis.

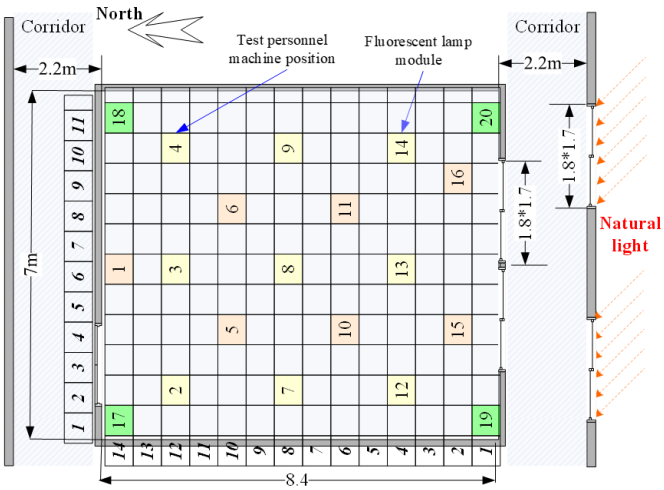

Figure 9. Test site modeling: Abstract representation of architectural and illumination layout

Furthermore, the following rules were applied for the illumination intensity measurement:

- The collection of illuminance data was conducted from 9 a.m. to 8 p.m., with measurements taken every hour.
- The data collection spanned two days, one set with the indoor lights turned on all day, and the other with all the lights turned off during the test.
- Illuminance intensity was measured in lux.

In accordance with the rules, measurements were carried out at the test points given in Figure 9. The graphical results of indoor illumination intensity are shown in Figures 10 and 11.

Through these measurements, changes in indoor illumination quantification at different times can be observed. Among them:

(1) Areas far from windows and thus from natural light experience small changes in illumination intensity, generally varying within the range of 90-120 lux.

(2) The light in the central area is relatively uniform, with fluctuations within the range of 130-170 lux.

(3) Areas near windows, influenced by natural light, experience dramatic fluctuations within the range of 400-2000 lux. The frequency of change is high; for instance, when sunlight is obscured by clouds, illumination can rapidly drop from 2000 lux to around 500 lux.

(4) The change pattern of illuminance between 10 a.m. and 5 p.m. is consistent with the sun's movement. Other periods are subject to less variation due to scattered light and the impact of artificial light sources.

(5) After turning off artificial light sources, the overall indoor illumination intensity drops to the level of 40-130 lux during the day (except near windows) and falls to zero at night. During this time, only the light produced by computer screens is present, averaging around 5-25 lux.

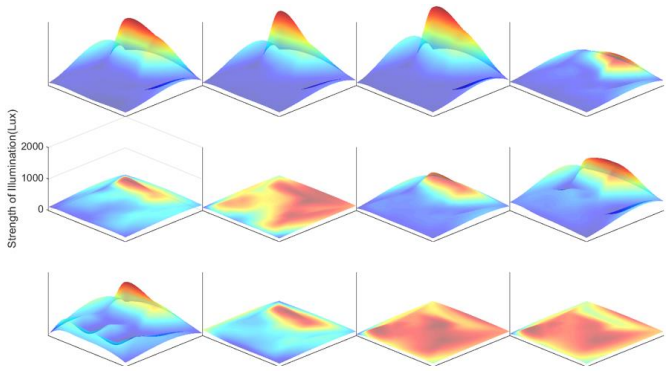

Figure 10. Measurement results of illuminance intensity: with artificial light source on

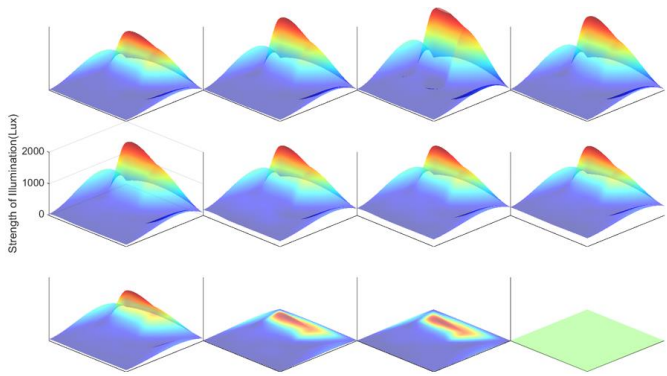

Figure 11. Second set of illuminance intensity measurement results: with artificial light source off

4.2 Monocular vision gaze point calibration

During the calibration process, six groups of participants were randomly selected from the subjects, including both males and females. As shown in Figure 12, nine marked points are represented by circles. During subsequent calibration, testers will observe calibration images appearing randomly from these nine locations. Each calibration point was displayed for three seconds, and after filtering out invalid data, an average of 30-40 gaze points could be collected for each calibration point.

In the tests, a 27-inch display with a resolution of 1920*1080 was used, and participants were approximately 50cm away from the screen. As shown by the red scattered points (gazing point) in Figure 12, the average gaze point error was less than 2.2cm, fully meeting the needs of subsequent attention test data collection. Furthermore, to compare

accuracy, the Tobii Eye [22] and aSee Pro desktop eye movement analyzers [24] were used during the calibration process.

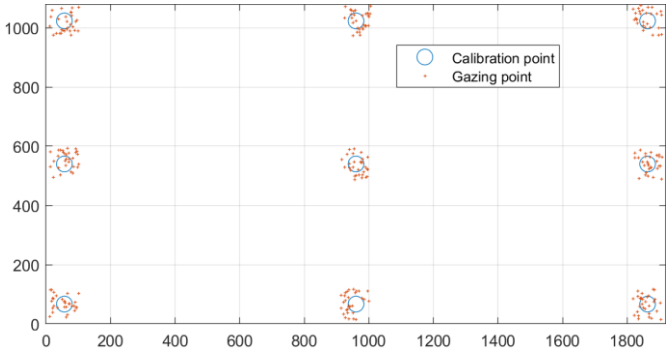

Figure 12. Gaze point calibration

4.3 Testing and data collection under different illumination conditions

4.3.1. Participant setup

For the focus data collection, nine university students aged 20-21 were selected, comprising five females g_1~g_5 and four males b_1~b_4. Their test positions are $P_{gril} = \{2,4,8,12,14\}$ and $P_{boy} = \{3,7,9,13\}$, respectively (as shown in shown in Figure 9), corresponding directly with the illumination intensity test points, thereby facilitating the establishment of an "Illumination Intensity-Attention" relationship model. After measuring the illuminance, participants began to run the CarSim program at their respective positions. Following the same sampling frequency and interval as in Section 4.2, each experimental group conducted 12 tests, each lasting approximately 300±10 seconds.

In addition, multiple drives on the same route by the same participant could result in accumulated driving experience, potentially leading to reduced attention due to experiential bias. To avoid this, 24 different road environments were selected for testing. Mapping the CarSim screen coordinate system to the plotting coordinate system allowed for the creation of gaze focus trajectory charts, providing an intuitive visualization process for analyzing participant attention and its changes-highlighting what the participant was focusing on at different times. The visualization results of a participant's focus trajectory from one of the tests are shown in Figure 5(b).

It can be observed that the majority (>97%) of the participant's attention was focused on the road, with a small portion allocated to the rearview mirror and the dashboard. However, a small amount exceeded the valid area. Based on this sample group, the participant's attention $Q' = 87.4\%$ can be calculated, indicating a high attention index.

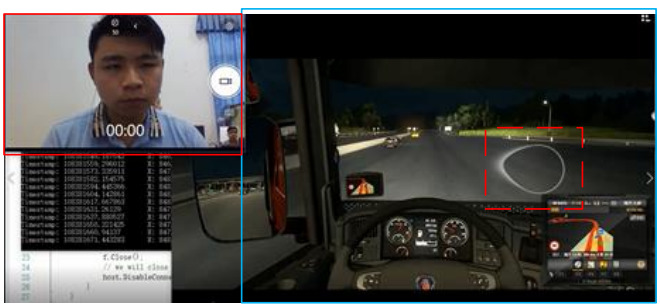

Figure 13. Test 1: Daytime environment

4.3.2 Testing in normal daylight conditions

For the test conducted under normal daylight conditions, a set of simulated driving samples was employed, from which focus data was obtained and observations were made. The specific test environment is displayed in Figure 13.

Region 1 is where the test participant was currently working, under daylight testing conditions, with no external disturbances set and no influencing factors related to the participant's attire (e.g., glasses, sunglasses). Regions 2 and 3 are elaborated on as in Section 3.2.

Upon completion of the daytime test, a set of gaze point plane trajectories was obtained, as shown in Figure 14.

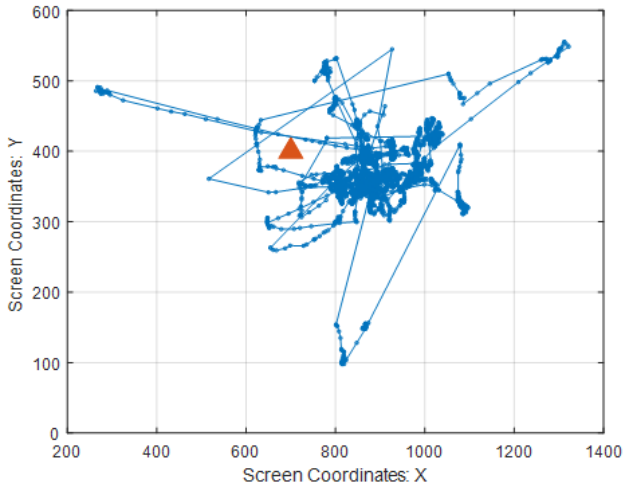

Figure 14. Test 1: Gaze point trajectory under daylight conditions

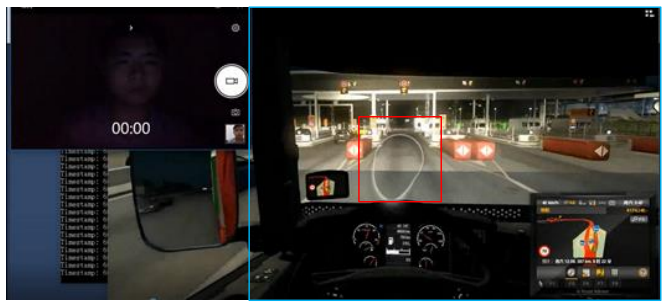

Figure 15. Test 2: Nighttime environment

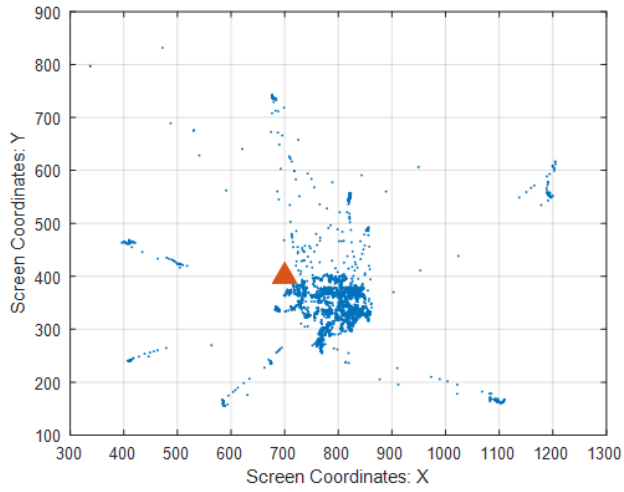

Figure 16. Test 2: Scatterplot of gaze points in the nighttime environment

4.3.3 Testing in nighttime conditions

In the simulated nighttime testing scheme, the test site lighting was turned off, leaving only the CarSim environment light (simulated by the display). The specific test environment is presented in Figure 15.

Figure 16 depicts the overall plane distribution image of gaze point movements during the nighttime test.

4.3.4 Testing in downlight conditions

An adjustable external lighting device was installed behind the test computer for illumination, following which tests were carried out on the computer running the samples. The specific test diagram is shown in Figure 17.

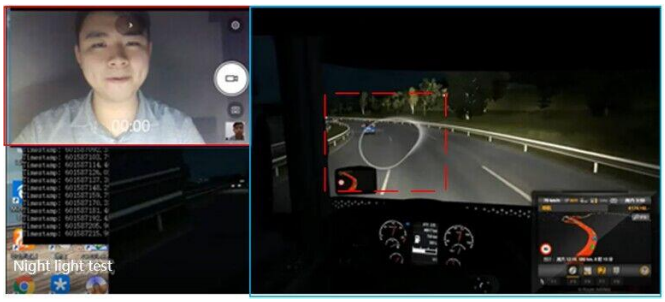

Figure 17. Test 3: Downlight testing environment

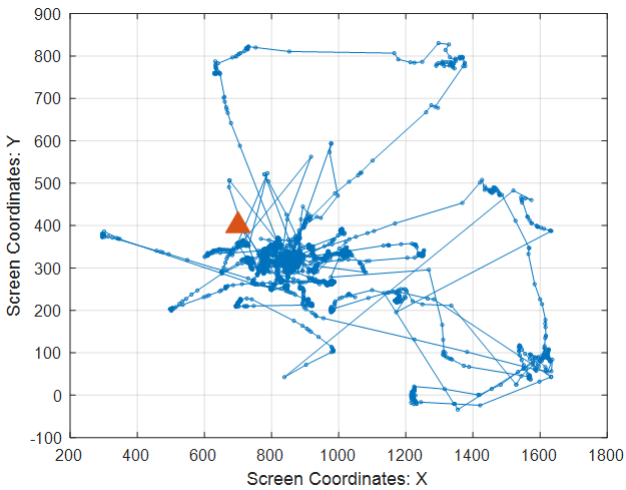

Figure 18. Test 3: Gaze point trajectory in downlight conditions

From Figure 18, it is discernible that during this test, the participant's gaze was primarily focused in the central region of 800-1000, with data outside the Y-axis 200 to 600 likely to be anomalies. Moreover, some anomalous data was concentrated around 1200-1600, indicating that the participant looked towards the bottom right corner more frequently in this experiment.

4.3.5 Testing in sidelight conditions

The lighting device was placed at a 45-degree angle from the test participant, directly irradiating the device, and then the samples were opened for recognition testing. The specific test environment is shown in Figure 19. In this environment, the overall lighting is brighter as shown in Figure 20, which helps testers concentrate on observing the roadway ahead (center). At the same time, the brighter lighting illuminates the rearview mirror (bottom left), which directs more attention of testers towards it.

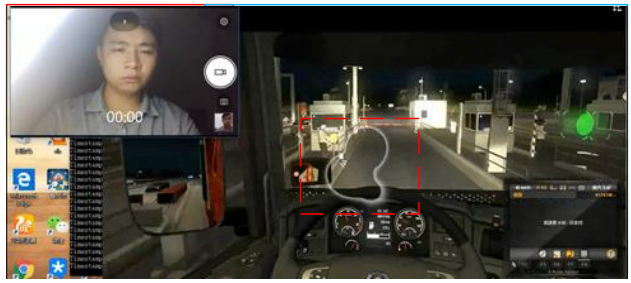

Figure 19. Test 4: Sidelight environment

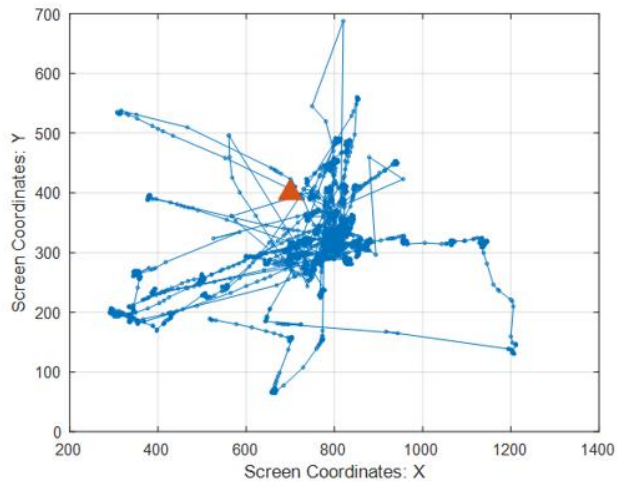

Figure 20. Test 4: Scatterplot of gaze points in sidelight conditions

4.4 Testing and analysis result

The testing and analysis results are conducted based on the attention quantification model proposed in section 3 and the illumination environment design and testing conditions outlined in section 4. The test data is described as follows:

•Illumination intensity data comprised 480 data points, distributed across 2 groups, 12 time periods, and 20 testing points, including 4 edge nodes and 16 measurement points.

•Focus data included 216 data entries across 2 groups, 12 time periods, and 9 individuals, including 4 men and 5 women. Each data entry contained about 9,000 focus samples, amounting to a total of approximately 1.944 million focus samples.

The focus data is converted into attention data, which provides a dataset for the relationship between illumination intensity and attention at each point. Fitting this data leads to the polynomial in Eq. (4), with an RMSE of approximately 2.9396. The comparison of the dataset is depicted in Figure 21.

The results of the testing reveal that:

•Overall, light intensity and attention have an inverse relationship; higher light intensities are more likely to cause disturbances in attention.

•When the light intensity is lower than 50 Lux, the external light source no longer plays a decisive role since it is either equivalent to or lower than the screen light intensity. As a result, the subjects' attention tends to hover near medium attention levels.

•On average, females exhibit slightly higher attention levels (88.84%) than males (88.08%). However, the distribution of the test results suggests that females have a better adaptive capability to light conditions.

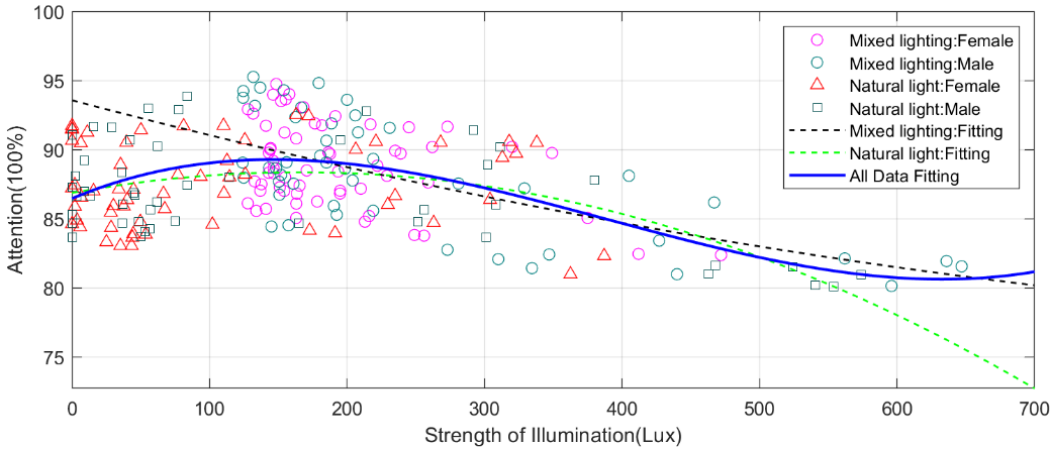

Figure 21. Comparison of test results

•Under natural lighting conditions, within the same range of light intensity (100300), the subjects' attention is essentially equivalent to that observed under artificial light sources.

•The overall attention is relatively high within the 100250 Lux light intensity. When the light intensity falls below this range, the average attention declines by about 1.2%.

•For the relationship equation of attention under mixed lighting, refer to Eq. (9); for the relationship equation of attention under natural light, refer to Eq. (10).

$$Q_p^{'} = 1.015\text{e-}05 \times \left(I_p\right)^2 + \text{-}0.02622 \times I_p + 93.56 \tag{9}$$

$$Q_p^{''} = \text{-}5.471\text{e-}05 \times \left(I_p\right)^2 + 0.01809 \times I_p + 86.86 \tag{10}$$

5. CONCLUSION

The article elucidated on the impacts of different lighting conditions on human attention, leveraging gaze point tracking under monocular vision to quantify the point of concentration of attention. An attention quantification model was built upon this, including a quantitative expression describing the relationship between lighting and attention. Both attention and behavioural traits of male and female subjects under diverse lighting conditions were compared, revealing how lighting conditions direct attention.

Appropriate lighting aids in maintaining prolonged attention, while darker environments facilitate greater focus on primary targets, like vehicles on the road, albeit they are also more susceptible to disruptions by secondary targets. Over-illumination leads to transient boosts in attention, yet these enhancements are unstable and short-lived. Conversely, the ability of males to sustain attention under high-intensity conditions is comparatively brief. This quantification assists in informing future research on human attention.

This model underwent comprehensive testing in the CarSim verification environment, with tested illumination levels generally not exceeding 700 Lux, a typical upper limit for bright indoor environments during summer and normal lighting conditions in classrooms and labs. Nevertheless, real-world lighting conditions can be more complex, for instance, direct summer sunlight can exceed 60,000 Lux, and overcast weather can reach up to 5,000 Lux, indicating a larger range of lighting variations that demand more complex lighting simulation environments. Hence, the effect of attention under stronger lighting conditions, such as high-intensity lighting environments in plateaus and ultrahigh-intensity environments of electric arc welding, are not included in this study, suggesting an important direction for future research.

In conclusion, the proposed lighting-attention model has significant implications for domains such as assisted driving, instructional design, and architectural lighting design. The rapid development of artificial intelligence in various fields has formed a huge pressure on the structural reform of China's labor supply side, especially the skilled and technical unemployment in the unemployment structure is difficult to control.The theory that productive forces determine the relations of production confirms the history and reality of the theory of "machines squeezing out workers" and the trend of "all-round development of man".

REFERENCES

[1] Baur, P., Iles, A. (2023). Inserting machines, displacing people: How automation imaginaries for agriculture promise 'liberation'from the industrialized farm. Agriculture and Human Values. https://doi.org/10.1007/s10460-023-10435-5

[2] Cooper, R.N. (1997). The general theory of employment, money, and interest. Foreign Affairs, 76(5): 217. https://doi.org/10.2307/20048216

[3] Schilirò, D. (2017). Economics versus psychology. Risk, uncertainty and the expected utility theory. Journal of Mathematical Economics and Finance, 1(4): 77-96. https://doi.org/10.14505/jmef.v3.1(4).04

[4] Jia, J., Zhang, H., Shi, B. (2022). Uncovering taxi mobility patterns associated with the public transportation shutdown using multisource data in Washington, DC. KSCE Journal of Civil Engineering, 26(12): 5291-5300. https://doi.org/10.1007/s12205-022-0434-5

[5] Mims, J.L. (2012). The eyes are the windows of the soul. Binocular Vision & Strabology Quarterly, Simms-Romano's, 27(4): 264-267.

[6] Chepesiuk, R. (2009). Missing the dark: Health effects of light pollution. Environmental Health Perspectives, 117(1): a20. https://doi.org/10.1289/ehp.117-a20

[7] Czeisler, C.A., Wright, K.P., Turek, F.W., Zee, P.C. (1999). Influence of light on circadian rhythmicity in humans. Lung Biology in Health and Disease, 133: 149-149.

[8] Kamali, N.J., Abbas, M.Y. (2012). Healing environment: Enhancing nurses' performance through proper lighting design. Procedia-Social and Behavioral Sciences, 35: 205-212. https://doi.org/10.1016/j.sbspro.2012.02.080
[9] van Duijnhoven, J., Aarts, M.P.J., Rosemann, A.L.P., Kort, H.S.M. (2018). Ambiguities regarding the relationship between office lighting and subjective alertness: An exploratory field study in a Dutch office landscape. Building and Environment, 142: 130-138. https://doi.org/10.1016/j.buildenv.2018.06.011
[10] Wood, B., Rea, M.S., Plitnick, B., Figueiro, M.G. (2013). Light level and duration of exposure determine the impact of self-luminous tablets on melatonin suppression. Applied Ergonomics, 44(2): 237-240. https://doi.org/10.1016/j.apergo.2012.07.008
[11] Jung, C.M., Khalsa, S.B.S., Scheer, F.A., Cajochen, C., Lockley, S.W., Czeisler, C.A., Wright Jr, K.P. (2010). Acute effects of bright light exposure on cortisol levels. Journal of Biological Rhythms, 25(3): 208-216. https://doi.org/10.1177/0748730410368413
[12] Bonmati-Carrion, M.A., Arguelles-Prieto, R., Martinez-Madrid, M.J., Reiter, R., Hardeland, R., Rol, M.A., Madrid, J.A. (2014). Protecting the melatonin rhythm through circadian healthy light exposure. International Journal of Molecular Sciences, 15(12): 23448-23500. https://doi.org/10.3390/ijms151223448
[13] Chen, Q., Ru, T.T., Zhou, J., Li, J., Xiong, X., Li, X., Zhou, G. (2018). The effects of light on social cognition and social behavior. Advances in Psychological Science, 26(6): 1083-1095. 10.3724/SP.J.1042.2018.01083
[14] Tanner, C.K. (2008). Explaining relationships among student outcomes and the school's physical environment. Journal of Advanced Academics, 19(3): 444-471. https://doi.org/10.4219/jaa-2008-812
[15] Guo, L., Zhang, X. (2017). Discussion on definition of healthy luminous environment and connection with standards. China Illuminating Engineering Journal, 28(6): 38-41. https://doi.org/10.3969/j.issn.1004-440X.2017.06.007
[16] Sandberg, M.A., Pawlyk, B.S., Berson, E.L. (1999). Acuity recovery and cone pigment regeneration after a bleach in patients with retinitis pigmentosa and rhodopsin mutations. Investigative Ophthalmology & Visual Science, 40(10): 2457-2461.
[17] Yang, C., Hu, H., Xiang, Y., Wang, T. (2018). Effects on visual fatigue of the human eyes of lighting parameters under LED luminous environment. Journal of Civil, Architectural & Environmental Engineering, 40(4): 88-93. https://doi.org/10.11835/j.issn.1674-4764.2018.04.013
[18] Dember, W.N., Neiberg, A. (1966). Individual differences in susceptibility to visual backward masking. Psychonomic Science, 6(2): 49-50. https://doi.org/10.3758/BF03327951
[19] Rasinski, T.V., Blachowicz, C.L., Lems, K. (2012). Fluency Instruction: Research-Based Best Practices. Guilford Press.
[20] Al-Qahtani, A., Nasir, A., Shakir, M.Z., Qaraqe, K.A. (2013). Cognitive impairments in human brain due to wireless signals and systems: An experimental study using EEG signal analysis. In 2013 IEEE 15th International Conference on e-Health Networking, Applications and Services (Healthcom 2013), Lisbon, Portugal, pp. 1-3. https://doi.org/10.1109/HealthCom.2013.6720780
[21] Wessel, J.R. (2018). Testing multiple psychological processes for common neural mechanisms using EEG and independent component analysis. Brain topography, 31: 90-100. https://doi.org/10.1007/s10548-016-0483-5
[22] Dalenberg, J.R., Hoogeveen, H.R., Lorist, M.M. (2018). Physiological measurements: EEG and fMRI. Methods in Consumer Research, 2: 253-277. https://doi.org/10.1016/B978-0-08-101743-2.00011-X
[23] Zheng, Z., Yang, J., Yang, L. (2005). A robust method for eye features extraction on color image. Pattern Recognition Letters, 26(14): 2252-2261. https://doi.org/10.1016/j.patrec.2005.03.033
[24] Park, K.R., Chang, J., Whang, M.C., Lim, J.S., Rhee, D.W., Park, H.K., Cho, Y. (2004). Practical gaze point detecting system. In Pattern Recognition: 26th DAGM Symposium, Tübingen, Germany, pp. 512-519. https://doi.org/10.1007/978-3-540-28649-3_63
[25] Kim, M.Y., Yang, S., Kim, D. (2012). Head-mounted binocular gaze detection for selective visual recognition systems. Sensors and Actuators A: Physical, 187: 29-36. https://doi.org/10.1016/j.sna.2012.08.016
[26] Gibaldi, A., Vanegas, M., Bex, P.J., Maiello, G. (2017). Evaluation of the Tobii EyeX Eye tracking controller and Matlab toolkit for research. Behavior Research Methods, 49: 923-946. https://doi.org/10.3758/s13428-016-0762-9
[27] De Tommaso, D., Wykowska, A. (2019). Tobiiglassespysuite: An open-source suite for using the tobii pro glasses 2 in eye-tracking studies. In Proceedings of the 11th ACM Symposium on Eye Tracking Research & Applications, Denver Colorado, pp. 1-5. https://doi.org/10.1145/3314111.3319828
[28] 7INVENSUN. https://www.7invensun.com/asee_pro.
[29] Wu, Y., Ji, Q. (2019). Facial landmark detection: A literature survey. International Journal of Computer Vision, 127: 115-142. https://doi.org/10.1007/s11263-018-1097-z
[30] Chen, F., Xu, Y., Zhang, D., Chen, K. (2015). 2D facial landmark model design by combining key points and inserted points. Expert Systems with Applications, 42(21): 7858-7868. https://doi.org/10.1016/j.eswa.2015.06.015
[31] Zhou, E., Fan, H., Cao, Z., Jiang, Y., Yin, Q. (2013). Extensive facial landmark localization with coarse-to-fine convolutional network cascade. In Proceedings of the IEEE International Conference on Computer Vision Workshops, Sydney, NSW, Australia, pp. 386-391. https://doi.org/10.1109/ICCVW.2013.58
[32] Satya Mallick.Facial Landmark Detection. https://learnopencv.com/facial-landmark-detection/#comment-2471797375.
[33] Seha, S.N.A., Hatzinakos, D., Zandi, A.S., Comeau, F.J. (2021). Improving eye movement biometrics in low frame rate eye-tracking devices using periocular and eye blinking features. Image and Vision Computing, 108: 104124. https://doi.org/10.1016/j.imavis.2021.104124
[34] Hacihaliloglu, I., Chen, E.C., Mousavi, P., Abolmaesumi, P., Boctor, E., Linte, C.A. (2020). Interventional imaging: Ultrasound. In Handbook of Medical Image Computing and Computer Assisted Intervention, pp. 701-720. https://doi.org/10.1016/B978-0-12-816176-0.00033-8
[35] Baker, C.A., Peterson, E., Pulos, S., Kirkland, R.A. (2014). Eyes and IQ: A meta-analysis of the relationship between intelligence and "Reading the Mind in the Eyes".

Intelligence, 44: 78-92. https://doi.org/10.1016/j.intell.2014.03.001
[36] Jian, M., Lam, K.M., Dong, J. (2014). Facial-feature detection and localization based on a hierarchical scheme. Information Sciences, 262: 1-14. https://doi.org/10.1016/j.ins.2013.12.001
[37] Zhang, H., Wang, J. (2015). Vehicle lateral dynamics control through AFS/DYC and robust gain-scheduling approach. IEEE Transactions on Vehicular Technology, 65(1): 489-494. https://doi.org/10.1109/TVT.2015.2391184
[38] Ebisawa, Y., Fukumoto, K. (2013). Head-free, remote eye-gaze detection system based on pupil-corneal reflection method with easy calibration using two stereo-calibrated video cameras. IEEE Transactions on Biomedical Engineering, 60(10): 2952-2960. https://doi.org/10.1109/TBME.2013.2266478
[39] Leclère, Q., André, H., Antoni, J. (2016). A multi-order probabilistic approach for Instantaneous Angular Speed tracking debriefing of the CMMNO14 ′ diagnosis contest. Mechanical Systems and Signal Processing, 81: 375-386. https://doi.org/10.1016/j.ymssp.2016.02.053
[40] Victory Instrument. http://www.china-victor.com/content/show/678/912.